Bifurcations of the self-consistent cranked harmonic oscillator

Eugene R. Marshalek
Department of Physics, University of Notre Dame, Notre Dame, Indiana 46556, USA
(Received 25 August 2003; published 29 December 2003)

The self-consistent cranked harmonic oscillator with volume conservation is examined more closely. Contrary to previous claims, bifurcations corresponding to tilted rotation are found to exist, even in systems with axially symmetric ground states. The tilted angular-momentum vector is proven to always lie in a principal plane of the ellipsoidal potential. The case of ^{20}Ne is used for illustrative purposes. Detailed graphical results are provided for the properties of the bifurcating trajectories, which are found with the aid of the cranked bifurcation theorem discussed in a previous publication.

DOI: 10.1103/PhysRevC.68.064308 PACS number(s): 21.60.Ev, 21.10.Re, 21.60.Jz, 47.20.Ky

I. INTRODUCTION

Since its introduction by Inglis in 1954 [1], the cranking model (CM) has been the main theoretical pillar for describing collective rotation in deformed nuclei. In the original version of the CM, the moment of inertia for low spins was obtained by summing the inertial effect of each particle as it is dragged around by a uniformly rotating deformed potential. Since then, it has evolved into the self-consistent cranking model (SCCM), which is a self-consistent uniformly rotating solution of time-dependent mean-field equations. Since the rotational motion in the SCCM is self-sustaining, the appellation "cranking model" is somewhat inappropriate but persists by tradition. Unlike the original CM, the SCCM is applicable to high-spin states, providing the chief theoretical backbone [2]. More recently, it has been shown that self-consistent cranking is not limited to the rotation of permanently deformed nuclei, but also provides a description of certain anharmonic vibrational bands [3]. The condition for applicability is that the nucleus must have at least one intrinsic C_∞ symmetry axis and that the vibrational mode carry nonzero angular momentum about this axis. According to the cranked bifurcation theorem (CBT) [3], when the nucleus is cranked about a symmetry axis, symmetry-breaking trajectories representing the vibrational bands bifurcate from axially symmetric states at critical points corresponding to the vanishing of random-phase approximation (RPA) frequencies in the rotating frame. These points are characterized by the angular velocities $\Omega=\omega_\mu/K_\mu$, where ω_μ is a collective vibrational RPA frequency (laboratory frame) for a mode built on an axially symmetric state projecting integer spin K_μ on the symmetry axis. The main purpose of this paper is to illustrate the consequences of this theorem using a mathematically tractable model.

An ideal testing ground is provided by the self-consistent cranked harmonic oscillator (SCCHO), especially in view of the elegant RPA analysis provided by Kurasawa [4] many years ago. The SCCHO itself has an old, but recently somewhat confusing history. In this model, nucleons move independently in a rotating three-dimensional anisotropic harmonic-oscillator potential, whose equipotentials maintain constant volumes while the potential frequencies are variationally optimized for each angular velocity. This volume-conservation (VC) constraint is intended to model nuclear incompressibility. It has been shown that under these circumstances, the potential is a true mean-field approximation to a peculiar internucleon interaction including two-body+three-body+$\cdots$+n-body+$\cdots$ interactions, where the two-body part is the "doubly stretched" quadrupole-quadrupole interaction [5–7]. The addition of certain embellishments, such as spin-orbit coupling and the pairing force, extends the SCCHO to a more realistic nuclear model, but with the sacrifice of mathematical transparency. The present paper is concerned with the pure SCCHO, which has some relevance for giant resonances. For most of its history, the SCCHO was applied only to rotation about a principal axis of the ellipsoidal potential, as reviewed in the textbook of Blaizot and Ripka [8]. Usually, the discussion was confined only to the ground-state band and its termination at an axially symmetric oblate state. A more systematic approach was attempted by Troudet and Arvieu [9], who found a new solution bifurcating from the terminal oblate state. Since the SCCHO system is not a rigid body (notwithstanding the rigid-body moment of inertia at low spins), one may ask whether the rotational motion is necessarily confined to a principal axis. If not, then one has the phenomenon of *tilted rotation*, i.e., rotation about an axis tilted with respect to a principal axis. In 1987, Cuypers [10] was the first to pose this question for the SCCHO. His conclusion was that the model only permits principal-axis (PA) rotation. Nevertheless, Heiss and Nazmitdinov [11] subsequently claimed to have found examples of tilted-axis (TA) rotation in the SCCHO. In a recent followup paper [12], these authors make the more specific statement: "A major outcome of the present paper is the result that, in even-even nuclei, tilted rotations occur if and only if the nucleus has a triaxial shape in its ground state." An inescapable implication of the present study is that both the conclusion of Cuypers and that of Heiss and Nazmitdinov are incorrect as shown by the example of ^{20}Ne. It should also be mentioned that in the past ten years, the topic of TA rotation has become a major focus of high-spin physics, both theoretically and experimentally [13]. The emphasis in this paper, however, will be on the SCCHO.

The SCCHO is first reviewed, with a derivation of the equations for rotational equilibrium close to that of Cuypers. It is then shown that if tilted rotations exist, the axis must be

confined to a principal plane. The equations are then applied to the case of ^{20}Ne, which has an axially symmetric prolate ground state and an axially symmetric oblate excited state. Bifurcations from these two states are found with the guidance of the CBT and the known RPA frequencies. Bifurcations corresponding to both PA and TA solutions are obtained, the former having $|K|=2$ and the latter $|K|=1$ as the spin projections on the symmetry axis. In order to obtain all the bifurcations, it is essential that the orbitals of the cranked oscillator be occupied diabatically. The properties of the trajectories at high spin are discussed in detail. Although the solutions appear as rotational equilibria, they are really superpositions of degenerate vibrations and therefore may be interpreted as anharmonic multiphonon vibrational bands. It is demonstrated that Cuypers' original equations have *pairs* of TA solutions bifurcating from the same point. An additional condition overlooked by Cuypers rules out one member of each pair as spurious. Ironically, not only do TA solutions exist, but there are too many of them.

II. FORMULATION OF THE SCCHO

A. Two rotating frames

The SCCM Hamiltonian (or Routhian) R in a frame rotating with angular velocity $\vec{\Omega}$ is given in general by

$$R = H_{\rm MF} - \vec{\Omega}\cdot\vec{L}, \tag{1}$$

where $\vec{L}$ is the angular momentum vector and $H_{\rm MF}$ is the mean-field Hamiltonian for A nucleons. For the SCCHO, $\vec{L}$ is assumed to be the *orbital* angular momentum, the intrinsic spin being taken into account only in the occupation of the single-particle levels. The mean-field Hamiltonian has the usual form

$$H_{\rm MF} = T + V = \sum_{i=1}^{A} [t(i) + v(i)], \tag{2}$$

where t is the kinetic energy, $t=\frac{1}{2}|\vec{p}|^2/m$, and v is the deformed potential for the ith nucleon. The Routhian may be defined relative to one of two reference frames. In one case, the reference frame coincides with the principal axes of v (PA frame), and in the second case with the direction of the angular momentum (spin frame). Thus, if one writes

$$R = \sum_{i=1}^{A} r(i) \tag{3}$$

and

$$\vec{L} = \sum_{i=1}^{A} \vec{\ell}(i), \tag{4}$$

the SCCHO single-particle Routhian in the PA frame, $r=r_{\rm PA}$, is given by

$$r_{\rm PA} = \frac{|\vec{p}|^2}{2m} + \frac{1}{2}m\mathring{\omega}_0^2\sum_{k=1}^{3}\omega_k^2 x_k^2 - \vec{\Omega}\cdot\vec{\ell}\,(\text{PA frame}), \tag{5}$$

where the potential is just the familiar three-dimensional anisotropic oscillator and the cranking term $\vec{\Omega}\cdot\vec{\ell}$ with $\vec{\ell}=\vec{r}\times\vec{p}$ allows for an arbitrary tilting of the angular momentum relative to the principal axes of the potential ("three-dimensional cranking"). The VC constraint requires that for any vector $\vec{\Omega}$, the oscillator frequencies obey the condition $\omega_1\omega_2\omega_3=1$. In the spin frame, the single-particle Routhian $r=r_{\rm s}$ is given by

$$r_{\rm s} = \frac{|\vec{p}|^2}{2m} + \frac{1}{2}m\mathring{\omega}_0^2\sum_{i=1}^{3}\sum_{j=1}^{3} k_{ij}x_i x_j - \Omega\ell_3\,(\text{spin frame}), \tag{6}$$

where the six parameters $k_{ij}(k_{ji}=k_{ij}, i\neq j)$ determine the shape and orientation of the potential tilted relative to the direction of the angular momentum. The VC condition in this case is obtained from the determinant of the symmetric matrix **k**:

$$\det \mathbf{k} = 1. \tag{7}$$

In Eq. (6), the direction of the angular momentum has arbitrarily been labeled as the three-direction in accord with Cuypers [10] ($\|\vec{\ell}\|=\ell_3$).

The two formulations, being related by a rotation of coordinates, are entirely equivalent. In both approaches, the rotating equilibrium solutions are obtained from the stationary variation of $\langle R\rangle$ with respect to the potential and orientation parameters, subject to the appropriate VC constraint. In practice, it was found that the use of the spin frame is more advantageous, both theoretically and numerically, in locating the bifurcation points, as well as providing more reliable convergence. In addition, the proof that the tilted angular momentum must lie in a principal plane of the ellipsoidal potential becomes trivial in this frame. Therefore, the spin frame will be used henceforth. Afterwards, the stationary solutions are rotated from the spin frame to the PA frame to provide the tilt direction and the intrinsic shape parameters of the oscillator potential in Eq. (5). The adopted intrinsic shape parameters are ϵ and γ, defined by [2]:

$$\omega_k = \omega_0(\epsilon,\gamma)\left[1 - \frac{2}{3}\epsilon\cos\left(\gamma + \frac{2\pi}{3}k\right)\right], \quad k=1,2,3, \tag{8}$$

where $\omega_0(\epsilon,\gamma)$ is chosen to secure the VC condition $\omega_1\omega_2\omega_3=1$. From now on, all energies will be measured in units of $\hbar\mathring{\omega}_0\simeq 41/A^{1/3}$ MeV, all frequencies in units of $\mathring{\omega}_0$, and all distances in units of $[\hbar/(m\mathring{\omega}_0)]^{1/2}$. This is tantamount to setting $\hbar=m=\mathring{\omega}_0=1$.

Since the single-particle Routhian in either frame is a quadratic form in coordinates and momenta, it may be diagonalized by a linear transformation to normal modes with the aid of a Bogoliubov transformation. The details for Eq. (6) are reviewed in the Appendix. Let $N_k\equiv B_k^\dagger B_k$ ($k=1,2,3$) be the normal-mode number operators, where $B_k^\dagger$, B_k are the boson creation and destruction operators, satisfying the usual com-

mutation rules $[B_\ell, B_k^\dagger]=\delta_{k\ell}$, $[B_\ell, B_k]=0$ (and H.c. equation). Then the diagonalized single-particle Routhian takes the form

$$r_s = \sum_{k=1}^{3} \varepsilon_k \left(N_k + \frac{1}{2} \right). \tag{9}$$

As shown in the Appendix, the normal-mode eigenfrequencies $\varepsilon = \varepsilon_k$ are roots of the polynomial equation

$$P(\varepsilon) \equiv (\varepsilon^2)^3 - a_4(\varepsilon^2)^2 + a_2\varepsilon^2 - a_0 = 0, \tag{10}$$

where

$$a_4 = k_{11} + k_{22} + k_{33} + 2\Omega^2,$$

$$a_2 = k_{11}k_{22} + k_{11}k_{33} + k_{22}k_{33} - (k_{12})^2 - (k_{13})^2 - (k_{23})^2 - \Omega^2(k_{11} + k_{22} - 2k_{33}) + \Omega^4,$$

$$a_0 = \det \mathbf{k} - \Omega^2[k_{11}k_{33} + k_{22}k_{33} - (k_{13})^2 - (k_{23})^2] + k_{33}\Omega^4, \tag{11}$$

and the determinant is explicitly given by

$$\det \mathbf{k} = k_{11}k_{22}k_{33} - k_{11}(k_{23})^2 - k_{22}(k_{13})^2 - k_{33}(k_{12})^2 + 2k_{12}k_{13}k_{23}. \tag{12}$$

It should be noted that $P(\varepsilon)$ is a cubic equation in ε^2. In order for a physical solution to exist, the roots of this cubic must all be real and positive. When this is the case, one must still choose the sign of each eigenfrequency ε_k. It is not true that all three eigenfrequencies must always be chosen positive, as assumed in previous papers. In fact, the correct sign is determined by the norm of the corresponding eigenvector as discussed in the Appendix, a point to be elaborated on further.

Assuming a fixed diabatic occupation, let $n_k(i)$ be the eigenvalue of N_k for the single-particle orbital occupied by the ith particle, and define the quantities Σ_1, Σ_2, and Σ_3 by

$$\Sigma_k \equiv \sum_{i=1}^{A} \left(n_k(i) + \frac{1}{2} \right), \quad k = 1, 2, 3. \tag{13}$$

Then the expectation value of the total Routhian (energy in the rotating frame), the sum of the individual contributions from Eq. (9), is given by

$$\langle R_s \rangle = \varepsilon_1\Sigma_1 + \varepsilon_2\Sigma_2 + \varepsilon_3\Sigma_3. \tag{14}$$

The rotating equilibrium solutions are those that are stationary with respect to variations of the parameters k_{ij} in $\langle R_s \rangle$, subject to the VC constraint (7). Therefore, defining the functional $F(\mathbf{k}, \Omega, \mu)$ by

$$F(\mathbf{k}, \Omega, \mu) \equiv \langle R_s \rangle - \mu \det \mathbf{k}, \tag{15}$$

where $\det \mathbf{k}$ is given by Eq. (12), and μ is a Lagrange multiplier (as is Ω), one obtains the equilibrium solutions from the set of six equations

$$\frac{\partial F(\mathbf{k}, \Omega, \mu)}{\partial k_{ij}} = \frac{\partial \langle R_s \rangle}{\partial k_{ij}} - \mu \frac{\partial \det \mathbf{k}}{\partial k_{ij}} = \Sigma_1 \left(\frac{\partial \varepsilon}{\partial k_{ij}} \right)_{\varepsilon=\varepsilon_1} + \Sigma_2 \left(\frac{\partial \varepsilon}{\partial k_{ij}} \right)_{\varepsilon=\varepsilon_2} + \Sigma_3 \left(\frac{\partial \varepsilon}{\partial k_{ij}} \right)_{\varepsilon=\varepsilon_3} - \mu \frac{\partial \det \mathbf{k}}{\partial k_{ij}} = 0 \tag{16}$$

together with the constraint (7). These equations can also be written in another form in terms of the cartesian components of the quadrupole tensor $Q_{\ell m}$:

$$Q_{\ell m} \equiv \left\langle \sum_{i=1}^{A} x_l(i) x_m(i) \right\rangle. \tag{17}$$

From the Hellmann-Feynman theorem [14] and Eq. (6), one then obtains

$$\frac{\partial \langle R_s \rangle}{\partial k_{ij}} = \left\langle \frac{\partial R_s}{\partial k_{ij}} \right\rangle = \frac{Q_{ij}}{1 + \delta_{ij}} \tag{18}$$

with the convention that all distances are measured in units of $[\hbar/(m\mathring{\omega}_0)]^{1/2}$. The Lagrange multiplier μ can be obtained from Eq. (16) and Euler's theorem on homogeneous functions, as follows:

$$\langle V_s \rangle = \sum_{i \geqslant j} k_{ij} \frac{\partial \langle R_s \rangle}{\partial k_{ij}} = \mu \sum_{i \geqslant j} k_{ij} \frac{\partial \det \mathbf{k}}{\partial k_{ij}} = 3\mu \det \mathbf{k} = 3\mu. \tag{19}$$

As shown by Cuypers [10], the virial theorem holds for the tilted oscillator, so that $\langle V_s \rangle = \frac{1}{2}\langle H_{\mathrm{MF}} \rangle \equiv \frac{1}{2}E$, where E is the total energy in the laboratory frame. Therefore

$$\mu = \tfrac{1}{6}E. \tag{20}$$

The total energy can also be written as

$$E = \langle R_s \rangle + \Omega \langle L_3 \rangle. \tag{21}$$

B. Equations for rotational equilibrium—analog of Riemann's theorem

From Eq. (16), the explicit evaluation of the conditions for rotational equilibrium requires the derivatives of the normal-mode frequencies with respect to the parameters k_{ij}. These can be obtained most simply by using Cuypers' implicit differentiation of the polynomial equation (10):

$$\frac{\partial \varepsilon}{\partial k_{ij}} = -\frac{\partial P / \partial k_{ij}}{\partial P / \partial \varepsilon}, \tag{22}$$

where, of course, k_{ij}, ε, and Ω are regarded as the independent variables. The derivatives are trivially calculated as, for example,

$$\frac{\partial P}{\partial \varepsilon} = 2\varepsilon(3\varepsilon^4 - 2a_4\varepsilon^2 + a_2), \tag{23}$$

where a_2 and a_4 are given by Eq. (11). Focusing for the moment on the derivatives with respect to the tilt param-

eters k_{ij} with $i \neq j$, one obtains

$$\frac{\partial P}{\partial k_{13}} = 2(k_{13}k_{22} - k_{12}k_{23} - k_{13}\Omega^2 - k_{13}\varepsilon^2), \tag{24a}$$

$$\frac{\partial \det \mathbf{k}}{\partial k_{13}} = 2(k_{12}k_{23} - k_{13}k_{22}). \tag{24b}$$

Furthermore,

$$\frac{\partial P}{\partial k_{23}} = 2(k_{23}k_{11} - k_{12}k_{13} - k_{23}\Omega^2 - k_{23}\varepsilon^2), \tag{25a}$$

$$\frac{\partial \det \mathbf{k}}{\partial k_{23}} = 2(k_{12}k_{13} - k_{23}k_{11}). \tag{25b}$$

Finally,

$$\frac{\partial P}{\partial k_{12}} = 2(k_{12}k_{33} - k_{13}k_{23} - k_{12}\varepsilon^2), \tag{26a}$$

$$\frac{\partial \det \mathbf{k}}{\partial k_{12}} = 2(k_{13}k_{23} - k_{12}k_{33}). \tag{26b}$$

Now, the definition of the spin frame is not unique. Given a solution of Eq. (16) characterized by a matrix $\mathbf{k}$, one can obtain another physically equivalent solution by performing an arbitrary static rotation about the 3-axis, which preserves the general form of Eq. (6). In particular, one may define a frame in which the condition

$$k_{12} = 0 \tag{27}$$

is satisfied, which simplifies everything, especially the equation $\partial F(\mathbf{k}, \Omega, \mu)/\partial k_{12} = 0$. From Eqs. (16), (18), and (26), this condition can be written either in the form

$$Q_{12} = 2\mu k_{13}k_{23}, \tag{28}$$

or, equivalently,

$$2k_{13}k_{23}\left[\Sigma_1\left(\frac{\partial P}{\partial \varepsilon}\right)^{-1}_{\varepsilon=\varepsilon_1} + \Sigma_2\left(\frac{\partial P}{\partial \varepsilon}\right)^{-1}_{\varepsilon=\varepsilon_2} + \Sigma_3\left(\frac{\partial P}{\partial \varepsilon}\right)^{-1}_{\varepsilon=\varepsilon_3} - \mu\right] = 0. \tag{29}$$

The Eq. (29) implies that either

$$k_{13}k_{23} = 0 \tag{30}$$

or else there exists a solution for which the quantity in brackets vanishes. For the latter possibility, however, Eq. (28) shows that $Q_{12} \neq 0$ if Eq. (30) does not hold, even though $k_{12} = 0$. This would violate the consistency between the mean-field potential and the density distribution, implying an unphysical solution. The conclusion then is that physical solutions must obey Eq. (30). These have the property that either k_{13} or k_{23} (or both) must vanish. If $k_{13} \neq 0$, then the angular momentum is tilted in the 1-3 principal plane of the ellipsoidal potential, while if $k_{23} \neq 0$, it is tilted in the 2-3 plane. The conclusion then is *physical solutions of the SCCHO have the property that the angular momentum must lie in a principal plane of the ellipsoidal mean field.*

This result is somewhat analogous to Riemann's theorem for a self-gravitating ellipsoidal fluid mass [15,16], which requires that the angular momentum (and vorticity) lie in a principal plane of the ellipsoidal mass distribution.

Although the treatment of the SCCHO generally follows that of Cuypers,[1] the last conclusion seems to have eluded him for two reasons. The first is that the condition $k_{12}=0$ was imposed by Cuypers as a constraint *before* the variation. Consequently, k_{12} never appeared as a variable, resulting in the automatic omission of the equation $\partial F(\mathbf{k}, \Omega, \mu)/\partial k_{12} = 0$ and its implications. Second, he seemed to have a bias against the existence of tilted solutions. This can be seen in the treatment of the equations corresponding to $\partial F(\mathbf{k}, \Omega, \mu)/\partial k_{13} = 0$ and $\partial F(\mathbf{k}, \Omega, \mu)/\partial k_{23} = 0$. The former equation, with $k_{12}=0$ taken into account, is explicitly given by

$$k_{13}\left\{\sum_{j=1}^{3}\left[\frac{(k_{22} - \Omega^2 - \varepsilon^2)\Sigma_j}{\varepsilon(3\varepsilon^4 - 2a_4\varepsilon^2 + a_2)}\right]_{\varepsilon=\varepsilon_j} - 2\mu k_{22}\right\} = 0, \tag{31}$$

while the latter equation can be obtained from it by exchanging $k_{13} \leftrightarrow k_{23}$ and $k_{11} \leftrightarrow k_{22}$, so that k_{23} factors out. Noting the existence of solutions with $k_{13}=k_{23}=0$ (as well as $k_{12}=0$), which corresponds to PA rotation, Cuypers immediately jumped to the conclusion that these are the *only* solutions. Unfortunately, he failed to consider the possibility that there might be solutions in which, for example, $k_{13} \neq 0$, but the expression in braces vanishes. In that case, of course, $k_{23}=0$, which would satisfy the companion equation, as well as Eq. (30). As shown by explicit calculations, such TA solutions indeed do exist, in addition to the usual PA solutions.

The situation, as it now stands, is that only four potential parameters need to be solved for: k_{11}, k_{22}, k_{33}, and either k_{13} or k_{23}. The exchanges $k_{13} \leftrightarrow k_{23}$ and $k_{11} \leftrightarrow k_{22}$ give physically equivalent solutions, as can be seen from Eqs. (24) and (25). The VC constraint reduces the number of parameters to three, while the Lagrange multiplier μ, as given by Eq. (20), can be expressed as a function of the other parameters.

Since the nonlinear equations are solved numerically for each value of the angular velocity Ω, the total angular momentum $\langle L_3 \rangle$, which is the true observable, can be calculated with the aid of the Hellmann-Feynman theorem as follows:

$$\begin{aligned}\langle L_3 \rangle = -\left\langle \frac{\partial R_s}{\partial \Omega} \right\rangle &= -\frac{\partial \langle R_s \rangle}{\partial \Omega} \\ &= -\Sigma_1\left(\frac{\partial \varepsilon}{\partial \Omega}\right)_{\varepsilon=\varepsilon_1} - \Sigma_2\left(\frac{\partial \varepsilon}{\partial \Omega}\right)_{\varepsilon=\varepsilon_2} \\ &\quad - \Sigma_3\left(\frac{\partial \varepsilon}{\partial \Omega}\right)_{\varepsilon=\varepsilon_3}.\end{aligned} \tag{32}$$

[1]Cuypers includes a correction for spurious center-of-mass motion that is omitted here since it is an A^{-1} correction, which is of the same order as other omitted A^{-1} corrections lying outside of the mean-field approximation.

The derivatives of the eigenfrequencies can be obtained by implicit differentiation of the polynomial equation (10) as follows:

$$\frac{\partial \varepsilon}{\partial \Omega} = -\frac{\partial P/\partial \Omega}{\partial P/\partial \varepsilon}, \tag{33}$$

where

$$\frac{\partial P}{\partial \Omega} = -2\Omega[2\varepsilon^4 + (k_{11}+k_{22}-2k_{33}-2\Omega^2)\varepsilon^2 - k_{22}k_{33} - k_{11}k_{33} + k_{13}^2 + k_{23}^2 + 2k_{33}\Omega^2], \tag{34}$$

assuming that $k_{12}=0$, which should also be taken into account in the expression (23) for $\partial P/\partial\varepsilon$.

III. BIFURCATION POINTS OF THE SCCHO

A. Bifurcation equations

According to the CBT [3], for a given *axially symmetric* mean-field reference state with corresponding RPA eigenmode frequencies ω_μ, the bifurcation points resulting from cranking about the symmetry axis should occur at the critical cranking frequencies $\Omega_c=\pm\omega_\mu/K_\mu$, $K_\mu\neq 0$ being the angular momentum projected by the RPA exciton on the symmetry axis. The two signs allow for time-reversal symmetry. The RPA modes with $K_\mu=0$ do not provide any bifurcations. Since the bifurcating trajectory represents repeated application of an exciton operator, the RPA mode must not be a pure particle-hole excitation, but should have sufficient collectivity to allow repeated application. Another caveat is that $\Omega_c=0$ (Goldstone mode) may not correspond to a bifurcating trajectory in the sense of the CBT if the associated RPA normal-mode operator is not a true exciton, but rather a constant of motion. Nevertheless, it is sometimes convenient to nominally regard such a mode as a bifurcation point if it corresponds to a terminus of a collective band generated by cranking *perpendicular* to a symmetry axis.

Consider now a fixed axially symmetric mean field with $\omega_1=\omega_2\equiv\omega_\perp$. Cranking about the symmetry axis (3-axis) with angular velocity Ω then provides the following three eigenfrequencies [root of Eq. (10)] of the Routhian:

$$\varepsilon_1=\omega_\perp+\Omega, \quad \varepsilon_2=\omega_\perp-\Omega, \quad \varepsilon_3=\omega_3 \tag{35}$$

with corresponding occupation factors $(\Sigma_1,\Sigma_2,\Sigma_3)$. Under these conditions, the variation of the Routhian with the VC constraint,

$$\frac{\partial}{\partial\omega_i}[\Sigma_1(\omega_\perp+\Omega)+\Sigma_2(\omega_\perp-\Omega)+\Sigma_3\omega_3-\mu\omega_\perp^4\omega_3^2]=0,$$

$$\omega_i=\omega_\perp,\omega_3 \tag{36}$$

yields the relation

$$\frac{1}{2}(\Sigma_1+\Sigma_2)\omega_\perp=\Sigma_3\omega_3=2\mu. \tag{37}$$

The associated angular momentum [Eq. (32)] is then given by

$$\langle L_3\rangle=\Sigma_2-\Sigma_1\equiv L_0. \tag{38}$$

Motivated by the CBT, one may seek bifurcations that break the symmetries at certain critical frequencies $\Omega=\Omega_c$. In order to find bifurcation points for *tilted* (TA) "rotation," set $k_{11}=k_{22}=\omega_\perp^2$, $k_{33}=\omega_3^2$, $k_{13}=0$, and assume $k_{23}\equiv\delta k_{23}\neq 0$ but infinitesimal (equivalently, one may take $k_{23}=0$ and $k_{13}\neq 0$). Then, Eq. (31) takes the form

$$\delta k_{23}\left[\frac{\Sigma_1+\Sigma_3}{\omega_3+\omega_\perp+\Omega_c}+\frac{\Sigma_2+\Sigma_3}{\omega_3+\omega_\perp-\Omega_c}+\frac{\Sigma_1-\Sigma_3}{\omega_3-\omega_\perp-\Omega_c}+\frac{\Sigma_2-\Sigma_3}{\omega_3-\omega_\perp+\Omega_c}-8\mu\omega_\perp\right]=0. \tag{39}$$

In order to have a tilted solution, the quantity in brackets must vanish giving

$$\frac{\Sigma_1+\Sigma_3}{\omega_3+\omega_\perp+\Omega_c}+\frac{\Sigma_2+\Sigma_3}{\omega_3+\omega_\perp-\Omega_c}+\frac{\Sigma_1-\Sigma_3}{\omega_3-\omega_\perp-\Omega_c}+\frac{\Sigma_2-\Sigma_3}{\omega_3-\omega_\perp+\Omega_c}=8\mu\omega_\perp=\frac{4\Sigma_3}{\omega_\perp}, \tag{40}$$

where the relation $\mu=\frac{1}{2}\omega_3\Sigma_3=\frac{1}{2}\Sigma_3/\omega_\perp^2$ from Eq. (37) and the VC constraint $\omega_\perp^2\omega_3=1$ were used in the last equality on the right-hand side. Apart from notational differences, Eq. (40) agrees completely with Kurasawa's [4] RPA equation for $|K|=1$ excitations built on axially symmetric states of the CHO, with the identification $\Omega_c=\omega_\mu$.[2] With a little algebra and the aid of Eqs. (37) and (38), the Eq. (40) can be written in the following simpler form:

$$\Omega_c\left[\Omega_c^3-\Omega_c(\omega_3^2+\omega_\perp^2)+\frac{L_0}{\Sigma_3}\right]=0. \tag{41}$$

The root $\Omega_c=0$, which represents a Goldstone mode (see Ref. [4]), does not correspond to a true bifurcation. Therefore, the bifurcation points for tilted rotation are in general the roots of the cubic equation

$$\Omega_c^3-\Omega_c(\omega_3^2+\omega_\perp^2)+\frac{L_0}{\Sigma_3}=0, \quad |K|=1 \tag{42}$$

with one qualification discussed in the following section.

Next, consider the bifurcation points for PA solutions, which project $|K|=2$ units of angular momentum on the symmetry axis. In this case, the relevant multipole of the mean field is proportional to $x_1^2-x_2^2$. Therefore, with the aid of Eqs. (16)–(18), set $k_{11}=\omega_\perp^2-\delta k_{22}$, $k_{22}=\omega_\perp^2+\delta k_{22}$, $k_{33}=\omega_3^2$, $k_{13}=k_{23}=0$, in the expression

$$\frac{1}{2}(Q_{11}-Q_{22})-\mu\left(\frac{\partial\det\mathbf{k}}{\partial k_{11}}-\frac{\partial\det\mathbf{k}}{\partial k_{22}}\right)=0. \tag{43}$$

The result is

[2]To go over to Kurasawa's notation, let $\Sigma_1\to\Sigma_-$, $\Sigma_2\to\Sigma_+$, $\Sigma_3\to\Sigma_1$, $\omega_3\to\omega_1$ [cyclic permutaion$(\omega_1\omega_2\omega_3)$]

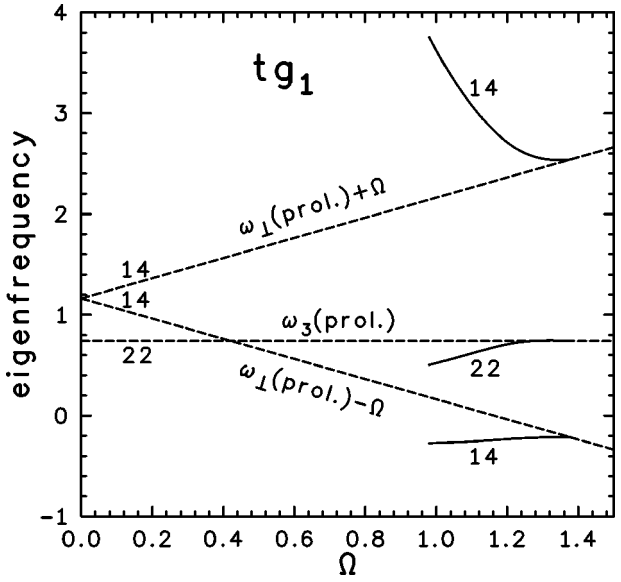

FIG. 1. Eigenfrequencies as a function of the rotational speed for the TA bifurcation from the ground state of ^{20}Ne. The vertical and horizontal axes are in units of $\mathring{\omega}_0$. The dashed lines are the eigenfrequencies for the prolate ground state cranked about the symmetry axis. The solid lines are the self-consistent eigenfrequencies for the symmetry-breaking bifurcation. The numerals 14, 14, 22 are the corresponding diabatic occupation sums.

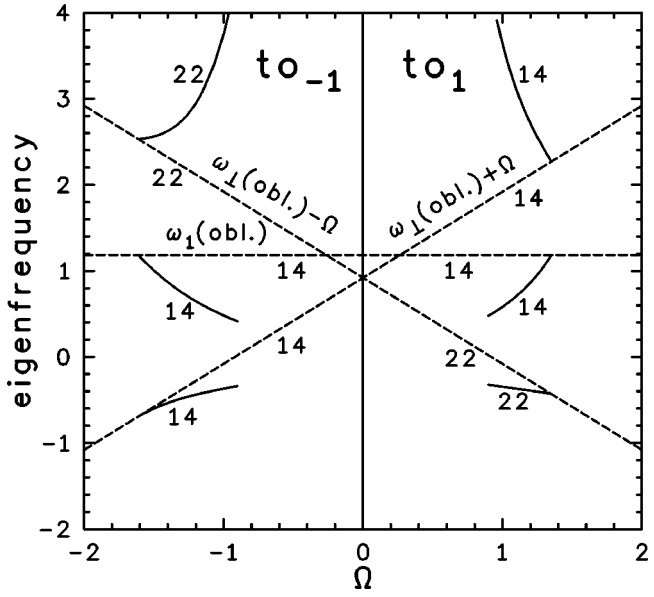

FIG. 2. Eigenfrequencies as a function of the rotational velocity for the two TA bifurcations from the oblate rotational band-termination state of ^{20}Ne. The vertical and horizontal axes are in units of $\mathring{\omega}_0$. The dashed lines are the eigenfrequencies for the oblate state cranked about the symmetry axis. The solid lines are the self-consistent eigenfrequencies for the symmetry-breaking bifurcation. The numerals 14, 14, 22 are the corresponding diabatic occupation sums.

$$\delta k_{22}\left[\frac{\omega_\perp \Sigma_1}{(\omega_\perp+\Omega_c)\Omega_c}-\frac{\omega_\perp \Sigma_2}{(\omega_\perp-\Omega_c)\Omega_c}+4\mu\omega_3\right]=0. \quad (44)$$

The nontrivial solution corresponds to the vanishing of the expression in brackets. With the aid of the second equality in Eq. (37) and the VC condition $\omega_\perp^2\omega_3=1$, the result can be written in the form

$$\frac{\Sigma_1}{\omega_\perp+\Omega_c}+\frac{\Sigma_2}{\omega_\perp-\Omega_c}+\frac{\Sigma_2-\Sigma_1}{\Omega_c}=4\omega_3^2\Sigma_3, \quad (45)$$

which agrees with Kurasawa's RPA equation for $|K|=2$ excitations, given the relation $\Omega_c=\omega_\mu/2$, which is in accord with the CBT. This can be equivalently written as the cubic equation

$$\Omega_c^3-\frac{1}{2}\omega_\perp^2\Omega_c+\frac{1}{4}\omega_\perp^6\frac{L_0}{\Sigma_3}=0, \quad |K|=2. \quad (46)$$

It should be noted that the replacement $\Omega_c\rightarrow-\Omega_c$ in Eqs. (42) and (46) has the same effect as $L_0\rightarrow-L_0$, equivalent to swapping Σ_1 and Σ_2. This just provides the (classical) time-reversed bifurcations. It will be sufficient to take $\Sigma_2\geqslant\Sigma_1$ so that the bifurcations are based on a mean-field state with $L_0\geqslant 0$.

The equations for the bifurcation points can be applied to either the axially symmetric oblate band-termination state, provided that $\Sigma_1\neq\Sigma_2$, ensuring that $L_0\neq 0$, or to an axially symmetric ground state, provided that $\Sigma_1=\Sigma_2$, implying $L_0=0$. In both cases, the symmetry axis has been arbitrarily labeled as the 3-axis to maintain the applicability of a single set of equations. Usually, the ground-state symmetry axis is labeled as the 3-axis, while the oblate symmetry axis is labeled as the 1-axis. This is because the ground and oblate states are connected by a finite rotational band of the ordinary kind, generated by cranking the ground state about an axis perpendicular to the symmetry axis (1-axis). The labeling is immaterial for observable properties. However, since relabeling involves permutation of the potential frequencies ω_1, ω_2, ω_3, it affects the assignment of the deformation parameter γ in Eq. (8). For this reason, the results are redefined according to the conventional labeling in extracting this deformation parameter in the calculations to follow. Also, in Figs. 1 and 2, the symmetry axis for the oblate state is labeled as ω_1(obl.).

B. The case of axially symmetric ground states

Systems with axially symmetric ground states are of special interest for two reasons. First, as will be demonstrated, one of the three roots of Eq. (42) does not correspond to a true bifurcation from the oblate band-termination state. Second, there is the claim of Heiss and Nazmitdinov [12] that such systems cannot have TA bifurcations, which is in disagreement with the present work.

In the case $\Sigma_1\neq\Sigma_2\neq\Sigma_3$, when the ground state of the nucleus is always triaxial, the Eq. (42) provides three genuine TA bifurcations based on the axially symmetric oblate band-termination state when such a state exists. The condition for the existence of such a state is $\Sigma_2/\Sigma_1\leqslant(\sqrt{27}+\sqrt{2})/(\sqrt{27}-\sqrt{2})$ [4,9]. The situation is different for a nucleus with an axially symmetric ground state, which always has an oblate band-termination state. The condition for this is the

equality of two occupation sums, say $\Sigma_1=\Sigma_3$. Then the bifurcation Eq. (42) depends only on the ratio $r=\Sigma_2/\Sigma_3$. The first equality in Eq. (37) and the VC constraint $\omega_\perp^2\omega_3=1$ imply that

$$\omega_3=\left(\frac{\Sigma_1+\Sigma_2}{2\Sigma_3}\right)^{2/3},\quad \omega_\perp=\left(\frac{2\Sigma_3}{\Sigma_1+\Sigma_2}\right)^{1/3}\text{(oblate)}. \quad (47)$$

From this, one infers that if $\Sigma_1=\Sigma_3$, then $r=2\omega_3^{3/2}-1$. In fact, Eq. (42) can be written entirely in terms of Ω_c and ω_3, which makes it easy to see that it factors as

$$(\Omega_c+\omega_\perp-\omega_3)[\Omega_c^2+(\omega_3-\omega_\perp)\Omega_c-2\omega_3\omega_\perp]=0. \quad (48)$$

The root $\omega_3-\omega_\perp$ is the energy of a pure particle-hole excitation as first noted by Kurasawa and therefore this does not correspond to a bifurcating trajectory. The roots of the residual quadratic equation are

$$\Omega_c(\pm)=\tfrac{1}{2}(\omega_\perp-\omega_3)\pm\tfrac{1}{2}\sqrt{(\omega_\perp+\omega_3)^2+4\omega_\perp\omega_3}, \quad (49)$$

which, in fact, do correspond to genuine TA bifurcation points. The point Ω_c $(-)$ clearly has a negative sign, which is entirely permissible, since a bifurcation carries spin that may be in the same or opposite direction to that of the reference state (pro and contra modes). Thus, Ω_c $(-)$ would be a contra mode and Ω_c $(+)$ a pro mode. Moreover, for each cranking solution, there is a (classical) time-reversed solution with opposite Ω, associated with the time-reversed reference state.

It is obvious from Eq. (49) that Ω_c $(+)>\omega_\perp$ for a TA bifurcation from the oblate band-termination state. In the case of a TA bifurcation from the ground state, Eq. (42) with $L_0=0$ explicitly yields the bifurcation points

$$\Omega_c(\pm)=\pm\sqrt{\omega_\perp^2+\omega_3^2}, \quad (50)$$

which correspond to degenerate time-reversal partners, so that it is sufficient to focus on the positive sign. In this case, the condition $\Omega_c(+)>\omega_\perp$ also holds. The Eq. (35) implies then that one of the eigenfrequencies of the SCCHO, namely, ε_2 is negative at the bifurcation point, and by continuity in some neighborhood of this point. Is a three-dimensional (cranked) oscillator with a real negative frequency unphysical? In the present context with a finite number of particles and a fixed diabatic occupation of the levels of the oscillator, the answer is not at all. As discussed in the Appendix, the diagonalization problem for the tilted CHO, having the same mathematical form as the RPA, requires that the sign of the eigenvalues be chosen according to the positive-norm criterion for the eigenvectors. For the eigenvalues in question, this automatically leads to the negative sign choice. In summary, for a nucleus with an axially symmetric ground state, the present study provides two TA bifurcation points Ω_c of different magnitude and opposite sign based on the oblate band-termination state with a given sign of the angular momentum. The replacement $\Omega_c\rightarrow-\Omega_c$ then gives the degenerate time-reversed solutions with opposite angular momentum. Based on the ground state, there is one bifurcation for $\Omega_c>0$, and a degenerate time-reversed bifurcation with the negative sign of Ω_c. In the case of a nucleus with a triaxial ground state, on the other hand, one expects three TA bifurcations based on the oblate band-termination state, if it exists, while for the ground state the CBT is inapplicable.

This brings up the assertion of Hess and Nazmitdinov [12] that the SCCHO does not permit TA solutions for a nucleus with an axially symmetric ground state, but admits one based on an oblate state of a triaxial nucleus. Although their argument seems nebulous, the essential part, given in an appendix, is the simple dictum that solutions for cranking frequencies Ω exceeding in magnitude any of the potential frequencies ω_1, ω_2, ω_3 are "unphysical," *even if the eigenfrequencies ε_j of the SCCHO are all real*. This criterion would render all the TA bifurcations points for the axially symmetric nucleus unphysical, but would admit the intermediate bifurcation for the triaxial nucleus. Although everyone agrees that a pair of complex values of ε_j cannot correspond to a physical solution, the disagreement here in effect is focused on the admissibility of a real but negative ε_j. As stated in the preceding paragraph, there is no reason to rule out such solutions in the present context. As shown in the following section, the numerical results are physically quite reasonable.

C. Bifurcation points for ^{20}Ne

Extensive SCCHO numerical computations have been performed for the celebrated nucleus ^{20}Ne, which has an axially symmetric prolate ground state and an axially symmetric oblate band-termination state. Assuming occupation of the orbitals by neutron-proton pairs, the set of occupation sums $\{\Sigma_1,\Sigma_2,\Sigma_3\}=\{14,14,22\}$ for the ground state. For the oblate band terminus, one has $\{\Sigma_1,\Sigma_2,\Sigma_3\}=\{14,22,14\}$ if the symmetry axis is labeled by ω_3. The frequencies of the oscillator potential for the oblate state are given by Eq. (47), while for the ground state they are given by

$$\omega_3=(\Sigma_1/\Sigma_3)^{2/3},\quad \omega_\perp=(\Sigma_3/\Sigma_1)^{1/3}\text{(ground state)}, \quad (51)$$

as follows from the self-consistency condition $\omega_\perp\Sigma_1=\omega_3\Sigma_3$, the VC constraint and $\Sigma_2=\Sigma_1$. Note that the $K=2$ bifurcation point from the ground state is just given by $\Omega_c=\omega_\perp/\sqrt{2}$, as follows from Eq. (46) with $L_0=0$. The critical bifurcation points for ^{20}Ne are given in Table I below.

The bifurcations are labeled as follows. The TA bifurcations are denoted by tg_K or to_K when based on the ground or oblate state, respectively. The PA bifurcations are denoted by pg_K or po_K when based on the ground or oblate state, respectively. The usual ground-state band, which is also a PA bifurcation from the oblate state, is denoted by the letter g. The TA bifurcations, which have broken r symmetry [13], correspond to a quantized sequence of angular momenta given by $L=L_0+nK$, where $K=\pm1$ and $n=0,1,2,\ldots$ is the number of vibrational phonons. The PA bifurcations, which have good r symmetry, also correspond to a quantized sequence of angular momenta given by $L=L_0+nK$, but with $K=\pm2$.

IV. NUMERICAL CALCULATIONS

All the bifurcating trajectories issuing from the ground and oblate states of ^{20}Ne were computed by numerically

TABLE I. The first column gives the reference state for the bifurcations, the second the angular momentum, the third and fourth, the potential frequencies perpendicular and parallel to the symmetry axis, respectively. The fifth column labels the bifurcations, as explained in the text, while the last column provides the critical bifurcation frequencies. Note that the zero-frequency terminus of the g band has been nominally included as a bifurcation point.

State	$L_0(\hbar)$	$\omega_\perp(\mathring{\omega}_0)$	$\omega_{\rm sym}(\mathring{\omega}_0)$	label	$\Omega_c(\mathring{\omega}_0)$
				tg_1	1.37804
Ground	0	1.16260	0.73984	pg_2	0.82208
				g	0.00000
				to_1	1.34917
				to_{-1}	−1.61192
Oblate	8	0.91964	1.18240	po_2	0.50005
				po_{-2}	−0.73514
				g	0.23509

solving the nonlinear equations discussed in Sec. II B for each value of the angular velocity Ω. These solutions represent rotating equilibrium states, although there is no guarantee that the equilibrium is stable. This question is briefly addressed in the concluding section. The eigenfrequencies ε_k of the SCCHO with the corresponding occupation sums for the tilted solutions are provided in Figs. 1 and 2.

It should be noted that the eigenfrequencies (solid lines) are provided only for the limited range of Ω values actually computed. The eigenfrequencies for the PA bifurcations could also have been included, but were omitted to avoid clutter. Figures 1 and 2 clearly show the diabatic occupation of the levels of the cranked axially symmetric system being inherited by the bifurcating levels. For TA solutions, one of the eigenfrequencies is always negative (as expected) because $\omega_\perp-\Omega$ or $\omega_\perp+\Omega$ become negative in the neighborhood of the bifurcation point.

Figure 3, showing the total angular momentum L ($\langle L_3\rangle$ or $\langle L_1\rangle$) plotted against the angular velocity Ω for all the bifurcating trajectories corresponding to the points in Table I, is the principal result of this paper.

The degenerate time-reverse bifurcations obtained from the replacements $\Omega\rightarrow-\Omega$, $L\rightarrow-L$ equivalent to rotating the figure by 180° have not been shown explicitly. Then, the oblate bifurcations occur from a state with $L_0=-8$. The three TA bifurcations tg_1, $to_{\pm1}$ have never been calculated before. The g band is just the familiar ground-state rotational band obtained by cranking the ground state *perpendicular* to the symmetry axis (three-axis), with the quantized spin sequence $L=0,2,\ldots,8$ and terminating at the oblate state. On the other hand, the g band is a legitimate bifurcation from the oblate state (in the sense of the CBT), obtained by cranking about the symmetry axis. The bifurcation po_2 was first found by Troudet and Arvieu [9], although the relation of the bifurcation point to the RPA frequency was not recognized at that time. The bifurcation pg_2 was first calculated by Marshalek and Nazmitdinov [17], while $po_{\pm2}$ were calculated by Marshalek [18]. A noteworthy feature is that the condition $dL/d\Omega>0$ is satisfied only for the g band and in a small

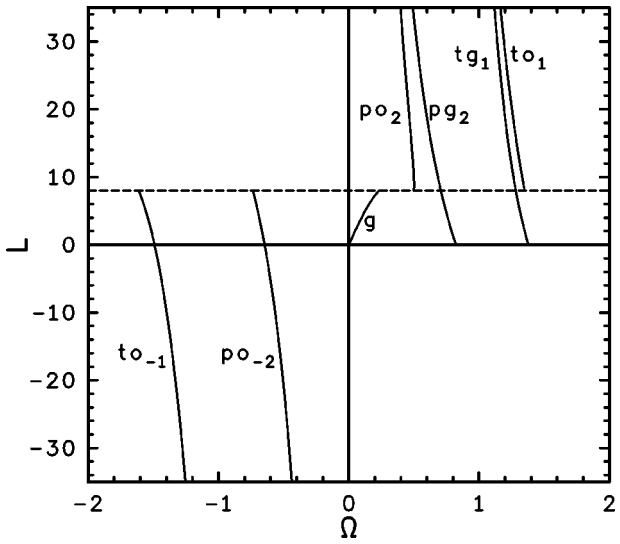

FIG. 3. Angular momentum L (units: $\hbar$) as a function of angular velocity Ω (units: $\mathring{\omega}_0$) for the bifurcations of ^{20}Ne. The horizontal solid line at $L=0$ represents the ground state, while the horizontal dashed line at $L=8$ represents the oblate state. The bifurcating curves are labeled according to conventions discussed in the text.

neighborhood of the bifurcation point of po_2; everywhere else $dL/d\Omega<0$, i.e., the trajectories exhibit backbending. All trajectories other than the g band extend to infinite magnitudes of L. The sequences to_{-1} and po_{-2} are especially interesting because the spins descend (although the energies increase), with L eventually becoming negative. This poses no problem in itself, since the degenerate time-reverse solution has positive L. Taking po_{-2} as an example, this implies the quantized spin sequence $L=8,6,\ldots,0,2,4,\ldots$. Thus, one has a descending followed by an ascending sequence of L values. Since the modes in question are of the contra type, this is not necessarily unphysical, but rather peculiar. On the other hand, as discussed in the concluding section, it is not clear that these solutions are truly stable equilibria in the ascending range.

A few words are in order concerning the backbending behavior in Fig. 3. The most familiar type of backbending in an L vs Ω plot is the *s*-shaped curve resulting from the quasicrossing of two rotational bands [2], which is rather different from the behavior in the present case. In the familiar case there is a steep increase in the moment of inertia over a small range of L or Ω as the adiabatic yrast sequence switches from the ground-state rotational band to the initially higher crossing band. In the present case, apart from a small region near the bifurcation point for po_2, L continually increases as Ω decreases, so that $L\rightarrow\infty$ as $\Omega\rightarrow0$, which, of course, implies a continual increase in the kinematic moment of inertia as the system approaches an elongated cylinder. Such behavior is well known for the rotational bifurcations of classical liquid drops, for example, the Jacobi sequence [19]. It should be kept in mind that the sequences discussed in the present work are really vibrational bands. When quantized, they correspond to overtone modes of the form $(1/\sqrt{n!})(\Gamma_\mu^\dagger)^n|L_0\rangle$, where $\Gamma_\mu^\dagger$ is a suitably defined phonon creation operator and $|L_0\rangle$ is the (correlated) reference state. For a purely harmonic

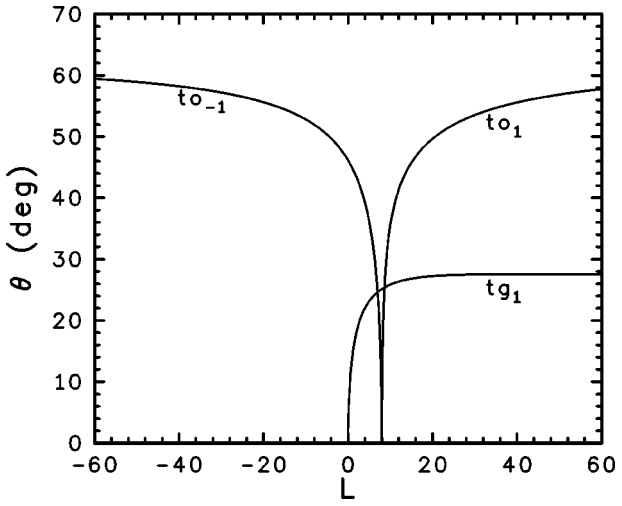

FIG. 4. The tilt angle θ (degrees) as a function of angular momentum L (units: $\hbar$) for the three TA bifurcating trajectories.

sequence, the energies would be given by $E=E_0(L_0)+(\omega_\mu/K_\mu)(L-L_0)$. Since $\Omega=dE/dL$, one would have $\Omega=\omega_\mu/K_\mu$=constant for the harmonic case. The corresponding curve in Fig. 3 would then be a vertical straight line. The backbending behavior, which implies that $d\Omega/dL=d^2E/dL^2<0$, reflects anharmonic effects. These anharmonicities imply a compression of the quantized spectrum, i.e., spacings between successive levels decrease. This effect can be seen in the energy diagram in Fig. 5 below. The energy for the purely harmonic limit is given by the tangent line at a bifurcation point while the actual anharmonic curve falls below this line.

Figure 4 plots the tilt angles of the three TA bifurcating trajectories as a function of the angular momentum. The tilt angle is always measured from the axis that corresponds to the symmetry axis at the bifurcation point. The portion of the $L<0$ curve for to$_{-1}$ could have been replaced by its time-reverse reflection with $L>0$, but this has not been done for esthetic reasons.

It should be noted that at the bifurcation points, $L=0$ for tg$_1$ and $L=8$ for to$_{\pm1}$, the tilt angles are all zero, and then rise very steeply with increasing magnitudes of L, eventually approaching saturation values of just below 30° for tg$_1$ and close to 60° for to$_{\pm1}$.

Figure 5 plots the excitation energies $\Delta E\equiv E-E_0$ of the bifurcating bands relative to the ground state as a function of angular momentum. This shows the g band and two other bifurcations branching from the ground state at $L=0$ and four bifurcations branching from the oblate terminus of the g band at $L=8$. The sequences to$_{-1}$ and po$_{-2}$ have increasing energy with decreasing angular momentum for $L>0$. Instead of smoothly continuing these curves for $L<0$, one may plot the degenerate time-reverse solution with positive $L>0$, as given by the two dashed lines. Then the sequence abruptly switches to one of increasing L with increasing energy. As mentioned before, there is some doubt as to whether these two solutions actually represent stable equilibria in this region.

Figure 6 portrays the deformation changes in terms of a plot of $\epsilon\sin\gamma$ vs $\epsilon\cos\gamma$ for each bifurcation, where the parameters ϵ and γ are defined by Eq. (8). The figure is largely self-explanatory. For the most part, the shapes are highly asymmetric. An interesting point is that an axially symmetric shape may momentarily evolve into another axially symmetric one, as illustrated by pg$_2$, which goes from prolate to oblate, and po$_2$, which goes from oblate to prolate. In principle, secondary CBT bifurcations from such axial shapes could occur. However, since the L values at which this occurs are not integers in general, the significance of such secondary bifurcations is not clear from a quantum viewpoint.

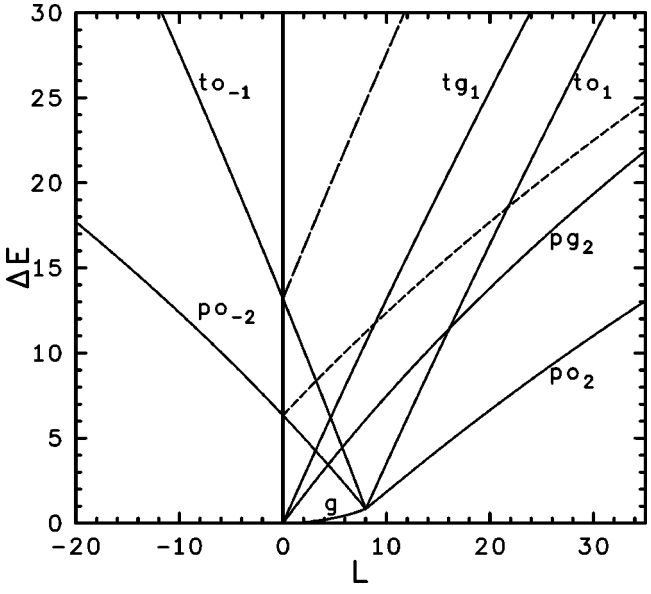

FIG. 5. The excitation energy ΔE (units: $\hbar\omega_0$) as a function of the angular momentum L (units: $\hbar$). The dashed curves are the time-reverse reflections of to$_{-1}$ and po$_{-2}$.

V. SUMMARY AND CONCLUSIONS

The present work serves three main purposes. First, it provides a microscopic illustration of the CBT, whose proof was based on perturbation theory in the neighborhood of the bifurcation points [3]. It is therefore reassuring to see that the bifurcating trajectories can be continued far from these points. The second purpose is to dispel some misconceptions concerning the SCCHO model. While Cuypers' [10] formulation of the conditions for rotating equilibrium is basically sound, his assertion that they do not admit tilted rotation is incorrect. Although Heiss and Nazmitdinov [11] realized this, they incorrectly concluded that TA rotation is possible only for systems with triaxial ground states [12]. The detailed numerical calculations for ^{20}Ne should dispel these misunderstandings. The third purpose is to provide a general proof that the TA solutions in the SCCHO must lie in a principal plane. A condition omitted in Cuypers' original formulation, given by Eq. (30), provides the key to a trivial proof. Figure 7 illustrates the additional importance of Eq. (30). It shows that without this condition unphysical tilted solutions exist with exactly the same bifurcation points as the

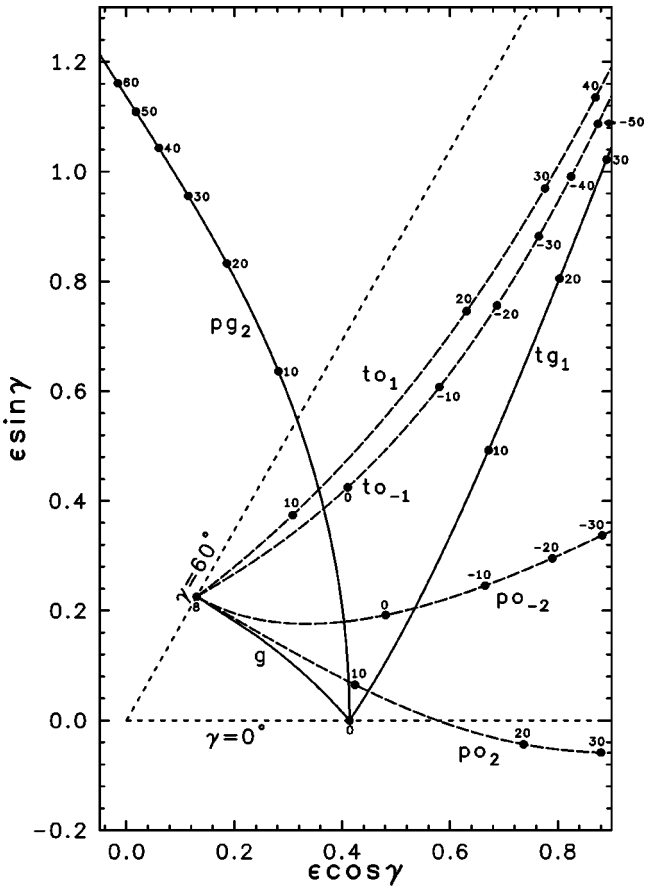

FIG. 6. $\epsilon \sin\gamma$ plotted against $\epsilon \cos\gamma$ for the bifurcating sequences. The straight dashed line at $\gamma=0°$ corresponds to axially symmetric prolate shapes, while that at $\gamma=60°$ to axially symmetric oblate shapes. Bifurcations from the ground state and the g band are represented by solid curves, while bifurcations from the oblate are represented by dashed curves. For each curve, the progression of L values (units: $\hbar$) at intervals of 10 is provided by the numbers accompanying the solid dots.

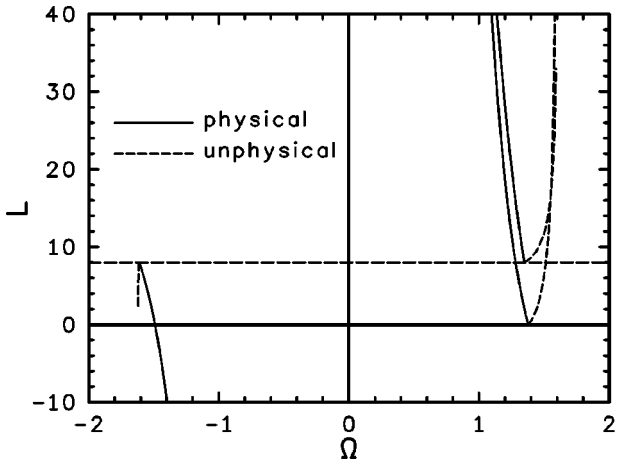

FIG. 7. The angular momentum L (units: $\hbar$) as a function of angular velocity Ω (units: ω_0) for the TA solutions. The physical solutions, which satisfy Eq. (30), correspond to the full curves, while the unphysical solutions, which violate Eq. (30), correspond to the dashed curves. The horizontal solid line at $L=0$ represents the ground state, while the horizontal dashed line at $L=8$ represents the oblate state.

physical tilted solutions. The unphysical solutions have the property that $k_{13}=k_{23}\neq 0$, which obviously violates Eq. (30).

It is interesting to note that while the physical solutions have the property $dL/d\Omega<0$ everywhere, the unphysical ones have the property $dL/d\Omega>0$.

An incidental observation of this work, is that a bifurcating trajectory may evolve from an axially symmetric prolate to oblate shape or vice versa, allowing for the possibility of secondary bifurcations via the CBT mechanism. This issue is left for future study.

In this paper, the nonlinear equations for rotating equilibria in the SCCHO model are solved numerically. The question of whether an equilibrium is stable or unstable has not been addressed. This could be done, for example, by solving the equations for the frequencies of RPA excitations built on the rotating mean-field solutions. Another possible approach is to check whether each stationary solution corresponds to an energy minimum. This is not quite so straightforward as it might seem. As is well known, solutions with the property that $dL/d\Omega<0$ (backbending) do not correspond to true minima of the total Routhian [Eq. (14)], but rather saddle points. Instead, one must seek minima of $\langle H_{\rm MF}\rangle$, the energy in the laboratory frame, *for fixed angular momentum*. Such a code was written, but found not to be as reliable nor as accurate as the one used for solving the nonlinear equations. Nevertheless, the former could be used to check if a solution of the latter is a local minimum. In this way, it was verified that all the physical bifurcations correspond to minima in some finite neighborhood of the bifurcation points, while none of the unphysical bifurcations passed this test. For the bifurcations with ascending values of the angular momentum L, a maximum value $L_{\rm max}$ seems to exist beyond which the minimizer could not find an energy minimum verifying the rotating equilibrium solution. Thus, for the bifurcation to_1, $L_{\rm max}\approx 28$, for po_2, $L_{\rm max}\approx 32$, and for pg_2, $L_{\rm max}\approx 12$. For the bifurcations with descending values of L, a minimum value $L_{\rm min}$ seems to exist. For the bifurcation to_{-1}, $L_{\rm min}\approx 1$, and for po_{-2}, $L_{\rm min}\approx 2$. In other words, the negative values of L appear to correspond to unstable equilibria. Fortunately, this would remove the paradox mentioned earlier. If the negative values were permitted, the degenerate time-reversed positive-L solution would imply a band with a descending followed by an ascending sequence of L values. It should be emphasized that the inability of the minimization code to locate a minimum within a designated range is not a rigorous criterion for instability — there may be delicate numerical reasons for this behavior. Therefore, the limits on L are very approximate. The tentative conclusion then is as follows: although the bifurcations have no limits on $|L|$, minimization for fixed L suggests that beyond a certain value of $|L|$, each bifurcation becomes unstable, probably via a saddle-point behavior. A rigorous conclusion would require the additional calculation of the RPA frequencies along the bifurcating trajectories, which is beyond the scope of this paper.

Finally, it may be worthwhile to recall the interpretation of the bifurcations, which is discussed in great detail in Ref.

[3]. While these bifurcations correspond classically to rotating equilibria obtained by superposing degenerate vibrations, from a quantal viewpoint they are multiphonon anharmonic vibrations. In particular, they represent overtone modes of the form $1/\sqrt{n!}(\Gamma_K^\dagger)^n|L_0\rangle$, where $\Gamma_K^\dagger$ is a suitably defined phonon creation operator and $|L_0\rangle$ is the (correlated) reference state. For more details, see Ref. [3]. In the case of the SCCHO, the bifurcations described in this paper represent quadrupole giant resonances built on either the ground or the oblate band-termination state, with the exception of the g band, which is the ordinary ground-state rotational band.

APPENDIX: DIAGONALIZATION OF THE CHO HAMILTONIAN

In order to diagonalize the single-particle CHO Routhian in the spin frame given by Eq. (6) with the units $\hbar=m=\mathring{\omega}_0=1$, it is convenient to first introduce the usual Cartesian creation and destruction operators $b_k^\dagger$, b_k via the transformation $x_k=(b_k^\dagger+b_k)/\sqrt{2}$, $p_k=i(b_k^\dagger-b_k)/\sqrt{2}$, $k=1,2,3$. The boson commutation rules $[b_k,b_\ell^\dagger]=\delta_{k\ell}$, $[b_k,b_\ell]=0$ (and Hermitian conjugate equation) correspond to the canonical commutation rules $[x_k,p_\ell]=i\delta_{k\ell}$, $[x_k,x_\ell]=0$, $[p_k,p_\ell]=0$. The Routhian then takes the general form

$$r_s=\tfrac{1}{2}\mathrm{tr}\mathcal{A}+\sum_{k=1}^{3}\sum_{\ell=1}^{3}\left[\mathcal{A}_{k\ell}b_k^\dagger b_\ell+\tfrac{1}{2}\mathcal{B}_{k\ell}(b_k^\dagger b_\ell^\dagger+b_\ell b_k)\right], \tag{A1}$$

where the matrices are explicitly given by

$$\mathcal{A}=\begin{pmatrix}\frac{1}{2}(k_{11}+1) & \frac{1}{2}k_{12}-i\Omega & \frac{1}{2}k_{13}\\ \frac{1}{2}k_{12}+i\Omega & \frac{1}{2}(k_{22}+1) & \frac{1}{2}k_{23}\\ \frac{1}{2}k_{13} & \frac{1}{2}k_{23} & \frac{1}{2}(k_{33}+1)\end{pmatrix},$$

$$\mathcal{B}=\begin{pmatrix}\frac{1}{2}(k_{11}-1) & \frac{1}{2}k_{12} & \frac{1}{2}k_{13}\\ \frac{1}{2}k_{12} & \frac{1}{2}(k_{22}-1) & \frac{1}{2}k_{23}\\ \frac{1}{2}k_{13} & \frac{1}{2}k_{23} & \frac{1}{2}(k_{33}-1)\end{pmatrix}. \tag{A2}$$

Both matrices are Hermitian, but $\mathcal{A}$ is complex while $\mathcal{B}$ is real. The CHO Routhian can be diagonalized in the form

$$r_s=\sum_{k=1}^{3}\varepsilon_k\left(B_k^\dagger B_k+\tfrac{1}{2}\right) \tag{A3}$$

by means of the Bogoliubov transformation

$$B_k^\dagger=\sum_{\ell=1}^{3}[u_\ell(\varepsilon_k)b_\ell^\dagger-v_\ell(\varepsilon_k)b_\ell], \tag{A4}$$

$$B_k=\sum_{\ell=1}^{3}[-v_\ell^*(\varepsilon_k)b_\ell^\dagger+u_\ell^*(\varepsilon_k)b_\ell].$$

The requirement that the normal-mode operators $B_k^\dagger$, B_k obey the usual boson commutation rules then leads to the following orthonormality conditions for the coefficients:

$$\sum_{m=1}^{3}[u_m(\varepsilon_k)u_m^*(\varepsilon_\ell)-v_m(\varepsilon_k)v_m^*(\varepsilon_\ell)]=\delta_{k\ell},$$

$$\sum_{m=1}^{3}[u_m(\varepsilon_k)v_m(\varepsilon_\ell)-u_m(\varepsilon_\ell)v_m(\varepsilon_k)]=0,\quad \text{(and H.c. equation)}. \tag{A5}$$

The equations of motion $[r_s,B_k^\dagger]=\varepsilon_k B_k^\dagger$ lead to the following 6×6 eigenvalue problem:

$$\begin{pmatrix}\mathcal{A} & \mathcal{B}\\ -\mathcal{B}^* & -\mathcal{A}^*\end{pmatrix}\begin{pmatrix}\underline{u}(\varepsilon_k)\\ \underline{v}(\varepsilon_k)\end{pmatrix}=\varepsilon_k\begin{pmatrix}\underline{u}(\varepsilon_k)\\ \underline{v}(\varepsilon_k)\end{pmatrix}, \tag{A6}$$

where $\underline{u}(\varepsilon_k)$, $\underline{v}(\varepsilon_k)$ are the three-dimensional column vectors whose respective components are the coefficients $u_k(\varepsilon_k)$, $v_k(\varepsilon_k)$. These equations have exactly the same mathematical form as the RPA eigenvalue problem. The equation for the eigenvalues obtained from

$$\det\left[\begin{pmatrix}\mathcal{A} & \mathcal{B}\\ -\mathcal{B}^* & -\mathcal{A}^*\end{pmatrix}-\varepsilon\mathcal{I}\right]=0, \tag{A7}$$

$\mathcal{I}$ being the six-dimensional identity matrix, is just Eq. (10).

The Eq. (A6) has the well known (and obvious) property that for each real eigenvalue (eigenfrequency) ε_k, its negative $-\varepsilon_k$ is also an eigenvalue with the associated eigenvector having the coefficients

$$u_\ell(-\varepsilon_k)=v_\ell^*(\varepsilon_k),\quad v_\ell(-\varepsilon_k)=u_\ell^*(\varepsilon_k). \tag{A8}$$

The normalization imposed by the first of Eqs. (A5), namely,

$$\sum_{m=1}^{3}[|u_m(\varepsilon_k)|^2-|v_m(\varepsilon_k)|^2]=1, \tag{A9}$$

can only be satisfied for one of the sign choices of ε_k because of a negative value of the sum for the other sign choice. It is important to check which sign choice yields an eigenvector for which the sum on the left-hand side is positive. Upon normalization, one then obtains the creation operator $B_k^\dagger$, with the operator $-B_k$ corresponding to the eigenvector associated to $-\varepsilon_k$, such that the condition $[B_k,B_k^\dagger]=1$ is satisfied. In other words, for a given $|\varepsilon_k|$, one sign choice defines the creation operator and the other the destruction operator. In the case of TA rotations of the SCCHO, there is always one eigenmode for which a negative value of ε_k defines $B_k^\dagger$.

[1] D. R. Inglis, Phys. Rev. **96**, 1059 (1954).
[2] Z. Szymański, *Fast Nuclear Rotation* (Clarendon, Oxford, UK, 1983).
[3] E. R. Marshalek, Phys. Rev. C **54**, 159 (1996).
[4] H. Kurasawa, Prog. Theor. Phys. **64**, 2055 (1980).
[5] E. R. Marshalek, Phys. Rev. C **29**, 640 (1984); Phys. Lett. B **244**, 1 (1990).
[6] T. Kishimoto *et al.*, Prog. Theor. Phys. Suppl. **74&75**, 170 (1983).
[7] H. Sakamoto and T. Kishimoto, Nucl. Phys. **A501**, 205 (1989); H. Sakamoto, *ibid.* **A557**, 583c (1993).
[8] J.-P. Blaizot and G. Ripka, *Quantum Theory of Finite Systems* (MIT Press, Cambridge, MA, 1985), pp. 146–151.
[9] T. Troudet and R. Arvieu, Ann. Phys. (N.Y.) **134**, 1 (1981).
[10] F. Cuypers, Nucl. Phys. **A468**, 237 (1987).
[11] W. D. Heiss and R. G. Nazmitdinov, Phys. Lett. B **397**, 1 (1997).
[12] W. D. Heiss and R. G. Nazmitdinov, Phys. Rev. C **65**, 054304 (2002).
[13] S. Frauendorf, Rev. Mod. Phys. **73**, 463 (2001).
[14] H. Hellmann, *Einführung in Die Quantumchemie* (Deuticke, Leipzig, 1937), p. 285; R. P. Feynman, Phys. Rev. **56**, 340 (1939).
[15] B. Riemann, Abh. Ges. Wiss. Göttingen **9**, 3 (1860).
[16] S. Chandrasekhar, *Ellipsoidal Figures of Equilibrium* (Yale University Press, New Haven, 1969), p. 129.
[17] E. R. Marshalek and R. G. Nazmitdinov, Phys. Lett. B **300**, 199 (1993).
[18] E. R. Marshalek, Phys. Rep. **264**, 279 (1996).
[19] R. A. Lyttleton, *The Stability of Rotating Liquid Masses* (Cambridge University Press, London, 1953), Chap. 4.